Direct current stimulation boosts synaptic gain and cooperativity *in vitro*

Asif Rahman 🆔, Belen Lafon, Lucas C. Parra and Marom Bikson

Department of Biomedical Engineering, The City College of The City University of New York, Steinman Hall, 160 Convent Ave, New York, NY 10031, USA

The Journal of Physiology

Key points

- Direct current stimulation (DCS) polarity specifically modulates synaptic efficacy during a continuous train of presynaptic inputs, despite synaptic depression.
- DCS polarizes afferent axons and postsynaptic neurons, boosting cooperativity between synaptic inputs.
- Polarization of afferent neurons in upstream brain regions may modulate activity in the target brain region during transcranial DCS (tDCS).
- A statistical theory of coincident activity predicts that the diffuse and weak profile of current flow can be advantageous in enhancing connectivity between co-active brain regions.

Abstract   Transcranial direct current stimulation (tDCS) produces sustained and diffuse current flow in the brain with effects that are state dependent and outlast stimulation. A mechanistic explanation for tDCS should capture these spatiotemporal features. It remains unclear how sustained DCS affects ongoing synaptic dynamics and how modulation of afferent inputs by diffuse stimulation changes synaptic activity at the target brain region. We tested the effect of acute DCS (10–20 V m^{-1} for 3–5 s) on synaptic dynamics with constant rate (5–40 Hz) and Poisson-distributed (4 Hz mean) trains of presynaptic inputs. Across tested frequencies, sustained synaptic activity was modulated by DCS with polarity-specific effects. Synaptic depression attenuates the sensitivity to DCS from 1.1% per V m^{-1} to 0.55%. DCS applied during synaptic activity facilitates cumulative neuromodulation, potentially reversing endogenous synaptic depression. We establish these effects are mediated by both postsynaptic membrane polarization and afferent axon fibre polarization, which boosts cooperativity between synaptic inputs. This potentially extends the locus of neuromodulation from the nominal target to afferent brain regions. Based on these results we hypothesized the polarization of afferent neurons in upstream brain regions may modulate activity in the target brain region during tDCS. A multiscale model of transcranial electrical stimulation including a finite element model of brain current flow, numerical simulations of neuronal activity, and a statistical theory of coincident activity predicts that the diffuse and weak profile of current flow can be advantageous. Thus, we propose that specifically because tDCS is diffuse, weak and sustained it can boost connectivity between co-active brain regions.

Introduction

Research into the cognitive and behavioural consequences of transcranial direct current stimulation (tDCS) has outpaced development of cellular models that can explain the diversity of applications, especially in the context of the unique spatiotemporal features of tDCS: sustained flow of weak direct current across large areas of the brain. Computational models of brain current flow during tDCS predict low intensity and diffuse current (Datta *et al.* 2009), which leads to sustained polarization of neurons across the brain (Rahman *et al.* 2015). Imaging studies confirm this diffusivity (Antal *et al.* 2012; Stagg *et al.* 2013). It has been speculated that the behavioural and clinical outcomes of tDCS reflect changes in connectivity between diffuse brain regions (Polania *et al.* 2011, 2012; Dasilva *et al.* 2012; Krishnamurthy *et al.* 2015). We provide data in support of a quantitative theory that diffuse and sustained brain polarization is advantageous in enhancing connectivity across brain regions.

Our theory is predicated on how tDCS changes ongoing synaptic function. Low-intensity direct current stimulation (DCS) produces a small change in membrane potential (<1 mV; Radman *et al.* 2009), which is not sufficient to induce spiking activity in resting cortical pyramidal cells. DCS, while weak, modulates synaptic efficacy at rest as measured by single evoked responses in humans (Nitsche & Paulus, 2000; Priori, 2003) as well as in animals (Bikson *et al.* 2004; Kabakov *et al.* 2012; Marquez-Ruiz *et al.* 2012; Rahman *et al.* 2013; Bolzoni & Jankowska, 2015; Jankowska *et al.* 2016). tDCS is typically applied adjunct to a task (corresponding to sustained neuronal activity) in clinical and performance enhancement applications. In these applications the endogenous activity is sustained for the task duration while tDCS is applied over the active brain region. However, the role of DCS on sustained synaptic activity between afferent presynaptic inputs and postsynaptic neurons is unclear. In what ways might the dynamics of ongoing synaptic activity enhance or dull the effects of DCS?

Any theory of tDCS mechanisms must explain the cellular targets of tDCS (Rahman *et al.* 2013), an idea we expand here to include afferent brain regions. Acute synaptic modulation by DCS has been linked to both polarization along the somato-dendritic axis (Jefferys, 1981; Bikson *et al.* 2004; Rahman *et al.* 2013) and afferent axon terminals (Hause, 1975; Kabakov *et al.* 2012; Rahman *et al.* 2013; Bolzoni *et al.* 2013*a*; Baczyk & Jankowska, 2014). Neuronal polarization does not have to be limited to just the target brain region during tDCS; activity in the target brain region can be modulated by the simultaneous polarization of neurons and their processes in afferent brain regions. Specifically, synaptic function in the target region will be determined by both local synaptic efficacy and afferent activity in terms of number of active axons and their firing rate – together these set the connectivity between the afferent region and the target. Specifically, during ongoing endogenous activity, connected brain networks that are coactive will be simultaneously polarized by the diffuse electric field (EF). We propose, DCS coupled with endogenous activity may modulate neuronal response in the target brain region through changes in afferent activity as a direct consequence of the diffuse current flow.

We quantified changes in synaptic efficacy in rat brain slices during constant and Poisson rate afferent synaptic activity. We assessed for the first time DCS modulation of synaptic efficacy during adaptation to ongoing activity and post-adaptation. Our experiments further identify a role for afferent axon polarization by DCS in driving ongoing activity. Experimental results are integrated into a model of connectivity between brain regions during tDCS which predicts that diffuse and sustained current flow increases the probability of coincident activity and endogenous plasticity between brain regions. Our findings suggest a specific substrate for how weak and diffuse DCS can amplify synaptic activity, modulate synaptic dynamics, and boost synaptic efficacy through cooperativity of afferent inputs.

Methods

Ethical approval

All animal experiments were carried out in accordance with guidelines and protocols approved by the Institutional Animal Care and Use Committee (IACUC) at The City College of New York, CUNY (Protocol No: 846.3).

Electrophysiology

Brain slices including a section of the primary motor cortex (M1) were prepared from male young adult Wistar rats aged 3 to 6 weeks old, which were deeply anaesthetized with ketamine (7.4 mg kg^{-1}) and xylazine (0.7 mg kg^{-1}) applied intraperitoneally (I.P.) and killed by cervical dislocation. The brain was removed and immersed in chilled (2–6°C) artificial cerebrospinal fluid (ACSF) containing (in mM): 126 NaCl, 4.4 KCl, 1.25 NaH$_2$PO$_4$, 2 MgSO$_4$, 2 CaCl, 24 NaHCO$_3$ and 10 D-glucose, bubbled with a mixture of 95% O$_2$–5% CO$_2$). A slightly modified ACSF composition was used for long-term plasticity experiments (1 mM MgSO$_4$). Coronal slices (400 μm thick) were cut using a vibrating microtome and transferred to a holding chamber for at least 30 min in ambient temperature. Slices were then transferred to a fluid–gas interface chamber perfused with warmed ACSF (30.0 $\pm$ 0.5°C) at 1.9 ml min^{-1}. The humidified atmosphere over the slices was saturated with a mixture

of 95% O_2–5% CO_2. Recordings started 1–3 h after dissection.

To probe synaptic efficacy, we stimulated the excitatory vertical pathway from L5A → 2/3 and the horizontal pathway within the superficial layers (L2/3). A recording electrode was placed 250–400 μm below the pial surface in L2/3 and a bipolar platinum/stainless steel stimulating electrode was positioned $\sim$500 μm vertically below it at the boundary of L3 and L5. Either 15 (in adaptation experiments) or 200 (in post-adaptation experiments) constant-current pulses (0.2 ms, 10–150 μA) were delivered at 5, 10, 20, or 40 Hz for constant train experiments with an interval of 60 s (15 pulse trains) or 4 min (200 pulse trains) between trains to allow for recovery from synaptic depression, from the refractory period, and from feed-forward or recurrent synaptic inhibition (however, potential mechanisms like post-activation depression may require a longer duration for recovery; Hultborn *et al.* 1996). Stimulus intensity was adjusted to produce responses half of the maximum amplitude that could be evoked. In a subset of experiments to evaluate the effect of DCS on a natural train of pre-synaptic action potentials, 81 pulses were delivered with Poisson distributed interspike intervals (4 Hz mean, 20 s). We also verified that the size of the stimulus artifact during DCS and during trains of orthodromic stimulation did not change.

Uniform extracellular EFs ($\pm$10 and 20 V m^{-1}) were generated by passing constant current (D/A driven analog follower; A-M Systems, WA, USA) between two large Ag–AgCl wires positioned in the bath across the slice starting 0.5 s before a train of constant or Poisson-distributed stimuli. In post-adaptation experiments, the field was applied after 100 pulses for 5 s that consisted of 50 pulses during DCS followed by another 50 pulses post DCS for a total of 200 pulses at a constant frequency of 10 Hz. Following clinical and brain slice conventions (Jackson *et al.* 2016), 'anodal' DCS corresponds to a positive electric field (positive electrode on motor cortex), while 'cathodal' DCS corresponds to a negative electric field (negative electrode over motor cortex). The quasi-uniform assumption (Bikson *et al.* 2012*a*), support this translational relevance of slice models. For all experiments, we used a Student's two-tailed *t* test to test for significance. In most cases we evaluated the significance between control and a DCS condition (anodal or cathodal DCS). In all cases the baseline refers to the magnitude of the field excitatory postsynaptic potential (fEPSP) prior to the onset of the train of afferent inputs or application of DCS.

Modelling synaptic dynamics and recruitment

The neuronal population response to excitatory pre-synaptic drive can be modelled as the averaged voltage response $V(t)$ (Richardson *et al.* 2005). A train of pre-synaptic spikes arriving down input fibre n over a large population of N_f input fibres at time t evokes excitatory postsynaptic potentials modelled as alpha synapses $\alpha(t)$.

$$V(t) = \sum_{n=1}^{N_f} \sum_{\{t_{nk}\}} A_k \alpha(t - t_k) . \qquad (1)$$

The set of amplitudes $\{A_k\}$, reflecting the field potential amplitudes, are modelled using a phenomenological description of dynamic synapses with short-term plasticity (Tsodyks & Markram, 1997; Mongillo *et al.* 2008). A simple quantitative model of postsynaptic response evoked by multiple synapses can be described as a product of a constant A_0 and two variables F and D:

$$A(t) = A_0 \cdot F(t) \cdot D(t) , \qquad (2)$$

$$\frac{dF(t)}{dt} = \frac{F_0 - F(t)}{\tau_F}, \, t = t_{AP} \Rightarrow F(t) \to F(t^-) + \Delta, \quad (3)$$

$$\frac{dD(t)}{dt} = \frac{1 - D(t)}{\tau_D},$$

$$t = t_{AP} \Rightarrow D(t) \to D(t^-)(1 - F(t^-)). \quad (4)$$

Synaptic efficacy is modulated by the amount of available resources D and the utilization parameter F that defines the fraction of resources used by each spike. The utilization parameter may reflect residual calcium level in the presynaptic terminal. Upon a spike, an amount FD of the available resources is used to produce the post-synaptic current, thus reducing D; physiologically the process mimics neurotransmitter depletion. The spike also increases F, mimicking presynaptic calcium influx. Experimentally, the field potential amplitude reflects the population averaged synaptic current and is well approximated by this model.

Between spikes, F and D exponentially recover to their baseline levels ($D = 1$ and $F = F_0$, $F \leq 1$) with time constants τ_F (facilitating) and τ_D (depressing). The phenomenological model reproduces behaviour of both facilitating ($\tau_F > \tau_D$) and depressing ($\tau_D > \tau_F$) cortical synapses.

We simulated a single postsynaptic integrate-and-fire neuron receiving correlated excitatory input signals. The cell received input through at most 1000 synapses during ongoing synaptic activity at a constant rate (10 Hz). To mimic glutamatergic transmission, synapses were conductance based with reversal potential $V_{Exc} = 0$ mV and time constant $\tau_{Exc} = 5$ ms. Additionally, every pre-synaptic spike leads to synaptic depression. Recruitment was modelled as an increase or decrease in the number of active synapses. The number of active synapses was

decreased from 1000 to 500 to simulate the dynamics during a decrease in synaptic cooperativity or increased from 500 to 1000 to simulate dynamics during an increase in synaptic cooperativity.

Statistical theory of coincident pre- and postsynaptic spikes

We present a statistical theory (eqn (5)) for increasing synaptic strength through changes in the likelihood of pre- or postsynaptic firing by considering the number of presynaptic spikes (N_{pre}) and the number of postsynaptic spikes (N_{post}) in discrete time bins (N_{bins}). The duration of each bin is taken to be 10–20 ms corresponding to the time constant of spike timing dependent plasticity. The hypergeometric distribution is used to estimate the coincidence count probability $P(k|N_{pre}, N_{post}, N_{bins})$ of observing k coincident pre- and postsynaptic spikes from a given number of bins and having observed N_{post} postsynaptic spikes and N_{pre} presynaptic spikes.

$$P\left(k|N_{pre}, N_{post}, N_{bins}\right) = \frac{\dbinom{N_{post}}{k}\dbinom{N_{bins} - N_{post}}{N_{pre} - k}}{\dbinom{N_{bins}}{N_{pre}}} .$$

(5)

Results

A quantitative description of synaptic dynamics during DCS predicts persistent changes in synaptic efficacy

The effects of DCS on online information processing in the brain can only be understood by considering synaptic dynamics during ongoing activity. A fundamental feature of synaptic transmission is adaptation to continuous afferent inputs (Abbott & Regehr, 2004), which is quantitatively described by short-term plasticity (eqn (1)). This established model for synaptic efficacy, which includes terms for synaptic gain and fibre number, is adapted here to describe the effects of DCS, for the first time. We begin with a consideration of DCS interactions with synaptic gain and then present data on fibre count.

Adaptation to synaptic activity arising from the depletion of neurotransmitters at the presynaptic terminal underlies important neural functions like gain control (Abbott *et al.* 1997) and working memory (Mongillo *et al.* 2008). The short-term plasticity phenomenon regulates synaptic efficacy and is quantified as a gradual decrease (for depressing synapses) or an increase (for facilitating synapses) in the excitatory postsynaptic potential (EPSP, Fig. 1*B*) during continuous presynaptic

inputs. Specifically, we quantified how DCS during presynaptic activity leads to a sustained change in the EPSP (eqn (1)). A conductance-based neuron model with dynamic synapses suggests that changes in postsynaptic membrane potential during DCS produces a sustained modification in EPSP amplitude and produces a greater net depolarization when anodal DCS is applied during ongoing synaptic activity (Fig. 1*C*). To test this prediction, we used an *in vitro* preparation where we could control the frequency of presynaptic inputs and study the effects of DCS on synaptic efficacy through the extracellularly recorded (field) EPSP (Fig. 2*A*), which we refer to simply as the field potential (FP).

DCS has a sustained and cumulative effect on synaptic efficacy

The effects of DCS on synaptic efficacy were evaluated during ongoing presynaptic activity in the rat primary
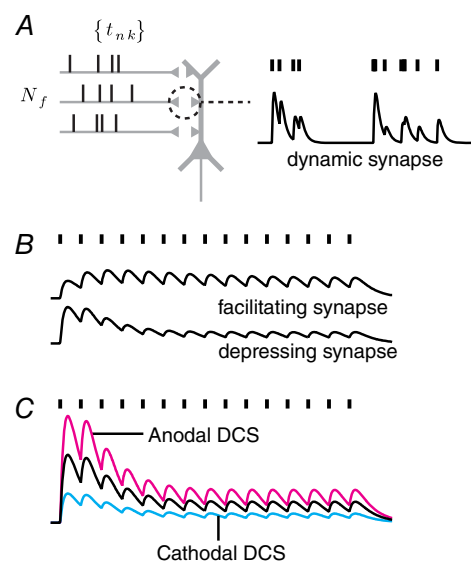

Figure 1. The postsynaptic voltage response during DCS and ongoing presynaptic activity results in sustained and cumulative changes that are regulated by synaptic efficacy, number of active inputs, and rate of presynaptic activity
A, schematic diagram representing the voltage output of a postsynaptic cell during a train of presynaptic spikes arriving at times {t_{nk}} down N_f input fibres. Synaptic transmission at cortical synapses are not static, but are dynamically regulated by the available pool of releasable vesicles. *B*, synaptic efficacy during activity is controlled by short-term plasticity based on the initial vesicle release probabilities ($P_{release}$) and vesicle depletion and recovery times. *C*, simulation of the postsynaptic response during DCS in a conductance-based model with dynamic synapses. Anodal DCS (magenta), modelled as a postsynaptic depolarization, facilitates EPSP amplitudes and cathodal DCS (blue), modelled as a postsynaptic hyperpolarization, depresses EPSP amplitudes. The postsynaptic response during DCS is sustained for the duration of DCS. [Colour figure can be viewed at wileyonlinelibrary.com]

motor cortex. Presynaptic afferent axons (L5A → 2/3 pathway) were stimulated at 5, 10, 20, and 40 Hz to simulate synaptic activity with field DCS applied in the anodal or cathodal direction (Fig. 2*A*). Field potentials (FPs) decayed in amplitude over the course of a 15 pulse train as a result of synaptic depression (defined as a gradual decrease in synaptic efficacy arising from adaptation mechanisms) (Fig. 2*B*). Anodal DCS increased ($+10$ V m^{-1}: $13.2 \pm 6.9\%$, $+20$ V m^{-1}: $20.3 \pm 9.8\%$, $n = 124$, $P < 0.05$) and cathodal DCS decreased (-10 V m^{-1}: $-13.3 \pm 8.7\%$, -20 V m^{-1}: $-23.3 \pm 11.2\%$, $n = 124$, $P < 0.05$) the first FP amplitude when applied during the train of inputs (Fig. 2*C*). Importantly, we show for the first time that the change in synaptic efficacy is maintained for the duration of DCS when there is a constant rate of synaptic inputs (Fig. 2*B* and *C*). The last FP amplitude during the train (referred to

as the steady-state FP amplitude), when the amplitude has reached a plateau, is significantly greater during anodal DCS and smaller during cathodal DCS, compared to the control case (no-DCS, Fig. 2*B* and *C*).

Computational models suggest there is cumulative membrane depolarization during ongoing synaptic activity and DCS may amplify the net depolarization (Fig. 1*C*). *In vitro*, DCS has a greater cumulative increase in synaptic efficacy during continuous presynaptic inputs. Anodal DCS increased and cathodal DCS decreased how fast the cumulative synaptic efficacy changed during synaptic activity, relative to baseline (Figs 2*F* and 3*C*). In slices with weak synaptic depression (referring to dynamics of synaptic transmission) or at low-frequencies of presynaptic input, anodal DCS can reverse synaptic depression towards facilitation for the duration of DCS. This finding is remarkable because it indicates DCS can
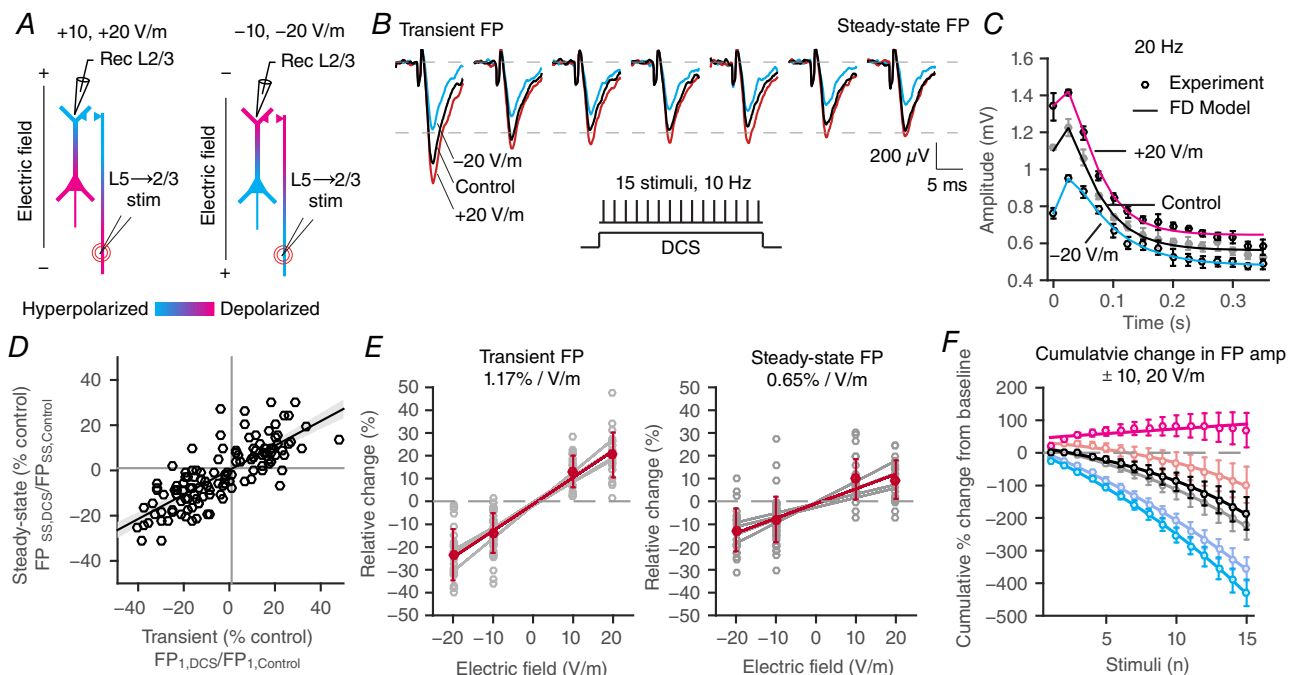
Figure 2. DCS in rat primary motor cortex results in a sustained modulation of synaptic efficacy
*A*, schematic diagram of anodal (left) and cathodal (right) DCS with current flow along the somato-dendritic axis and the effective membrane polarization of cells and axons in false colour. *B*, orthodromic stimulation of the L5 → 2/3 pathway at a constant frequency (20 Hz shown) in M1 facilitates synaptic efficacy during anodal DCS and depresses efficacy during cathodal DCS, compared to control cases without DCS (red: anodal, blue: cathodal, black: control, no DCS). The DCS effects are sustained for the duration of the electric field (EF). *C*, DCS modulates synaptic efficacy during continuous afferent inputs despite synaptic depression arising from vesicle depletion in the presynaptic terminals. *D*, the immediate change in field potential (FP) amplitude during DCS is correlated with the last FP amplitude during the train. Panel *D* shows FP amplitudes normalized by the corresponding *n*-th FP amplitude during a train without DCS. *E*, the sensitivity (% change in FP amplitude per V m^{-1}) to DCS of the last FP is less than the sensitivity of the first FP ($n = 124$) during the train. Grey best fit lines are for each of the tested frequencies (5, 10, 20, and 40 Hz) and red is the combined average across frequencies. There was no significant difference in sensitivities in either first or last FP across frequencies. *F*, the rate of cumulative change in FP amplitude (the cumulative % change from baseline) is greater during anodal DCS and less during cathodal DCS compared to control. Dark points indicate 20 V m^{-1} and light points are 10 V m^{-1}. In all cases, magenta indicates anodal DCS and blue is cathodal DCS (error bars are standard error). [Colour figure can be viewed at wileyonlinelibrary.com]

qualitatively change the nature of gain control in a given brain region, turning depressive dynamics into facilitating ones.

DCS produces frequency-independent changes in synaptic efficacy

A model of dynamic synaptic transmission consisting of a facilitating (F) and a depressing (D) term with first-order decay kinetics (referred to as the FD model) was fitted to the data and predicted the observed EF

effects. The most common form of short-term plasticity (>82% of experiments) observed in the rat primary motor cortex was short-term depression ($\tau_D > \tau_F$, $\tau_D = 0.74$ s, $\tau_F = 0.23$ sec, $F_0 = 0.18$, $\Delta = 0.41$). DCS had no effect on the time constants for depression or facilitation (Wilcoxon signed-rank test, $P > 0.05$), suggesting DCS does not have a direct effect on presynaptic transmitter release kinetics. Both in our experiments and in the FD model, ongoing synaptic activity results in a substantial reduction in FP amplitude due to synaptic depression. The change in synaptic efficacy resulting from DCS (and
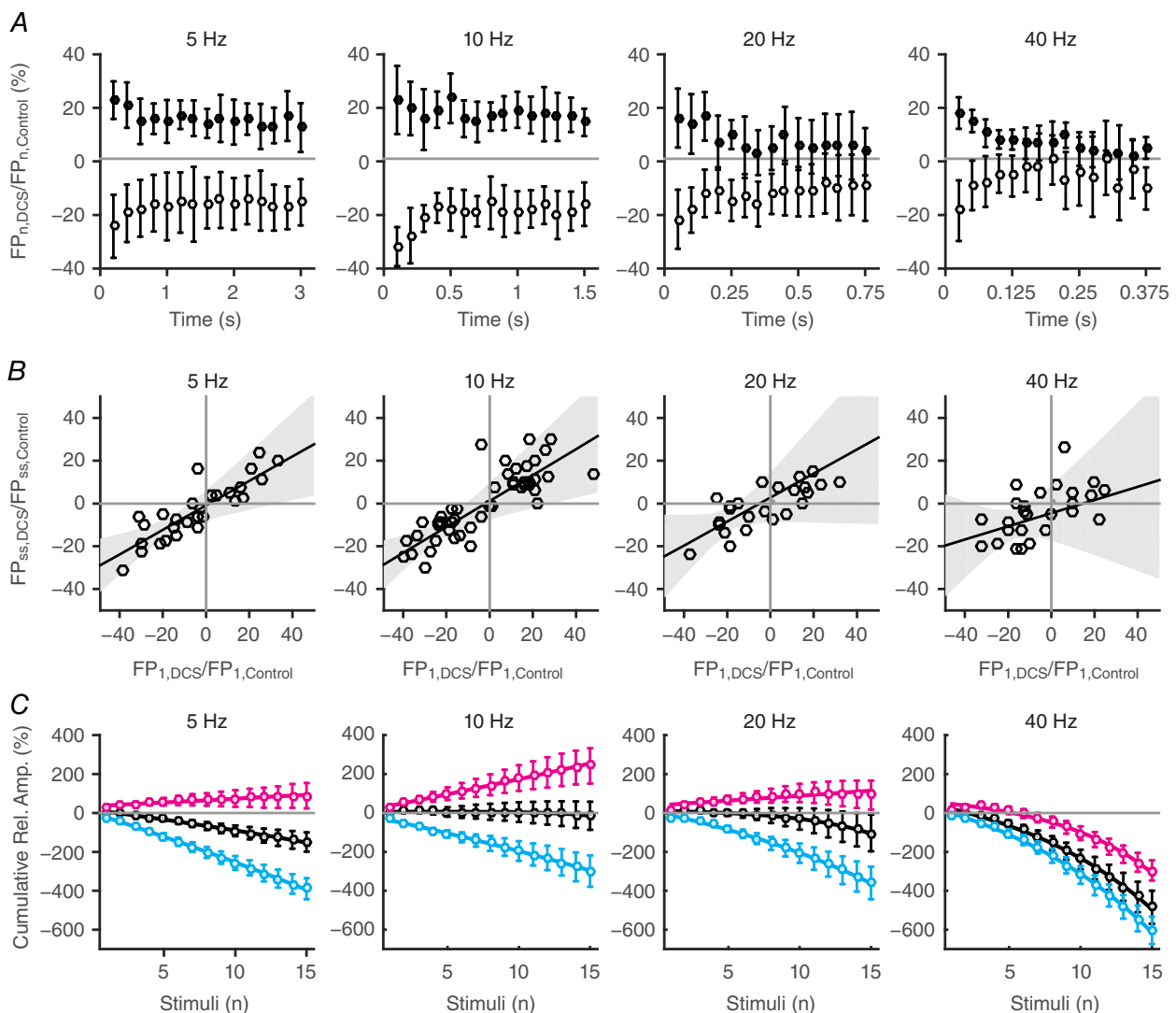
Figure 3. Synaptic efficacy is frequency-independently modulated during DCS, sustained for the duration of the electric field (EF), and is cumulative

A, the effect of DCS on synaptic efficacy is sustained during the trains at a constant rate of input. Here, FP amplitudes during DCS are normalized by the corresponding *n*-th FP amplitude in a control train, within slice (filled circles: anodal DCS, +20 V m^{-1}; open circles: cathodal DCS, −20 V m^{-1}). *B*, the immediate change in FP amplitude (*x*-axis, FP$_{1,\text{DCS}}$/ FP$_{1,\text{Control}}$) is correlated with the steady-state change in FP amplitude (*y*-axis, FP$_{\text{SS,DCS}}$/ FP$_{\text{SS,Control}}$, where SS refers to the FP amplitude at steady state). *C*, anodal DCS attenuates synaptic depression. The cumulative percentage change from baseline is plotted for anodal (magenta), cathodal (blue), and control (black) conditions. DCS can, in some cases, reverse synaptic depression. [Colour figure can be viewed at wileyonlinelibrary.com]

independent of synaptic depression) is quantified by normalizing each *n*-th FP amplitude during DCS ($FP_{n,DCS}$) by the corresponding *n*-th FP amplitude without DCS ($FP_{n,Control}$), within slice. The normalization reveals a sustained increase of synaptic efficacy with anodal DCS and decrease with cathodal DCS for as long as the EF is on (Fig. 3*A*). The sustained change in synaptic efficacy is frequency independent and persists during a naturalistic pattern of synaptic activity (Fig. 4).

Ongoing synaptic activity changes the synaptic sensitivity to DCS

There is a marked decrease in the sensitivity to DCS over time, quantified as the percentage change in FP amplitude from control per V m^{-1}, from 1.17 ± 0.1% per V m^{-1} to 0.65 ± 0.05% per V m^{-1} during ongoing synaptic activity (Fig. 2*E*). This change in sensitivity is independent of the rate of synaptic activity (Fig. 2*E*, grey lines indicate different rates of afferent synaptic inputs; rate coefficients: first FP: 0.03 ± 0.06% per V m^{-1}; steady-state FP: −0.03 ± 0.07% per V m^{-1}). Furthermore, the immediate and steady-state change in synaptic efficacy is directly correlated, across all frequencies (Figs 2*D* and 3*B*). Synaptic adaptation, therefore, reduces the capacity for DCS to modulate synaptic efficacy.

DCS modulates synaptic efficacy post adaptation

Modulation of synaptic efficacy after the adaptation period was measured by applying a long-duration train of 200 stimuli at 10 Hz (Fig. 5*A*); 20 V m^{-1} EFs were applied for 5 s after the first 100 pulses in the train. During DCS, synaptic
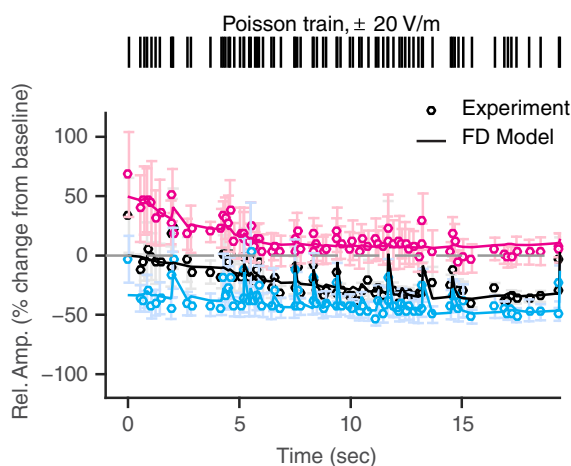
Figure 4. DCS produces a sustained change in synaptic efficacy during a naturalistic pattern of presynaptic activity
Afferent inputs reflecting the Poisson distributed spike train pattern *in vivo* (mean rate 4 Hz) is acutely facilitated by anodal DCS (magenta) and depressed by cathodal DCS (blue). [Colour figure can be viewed at wileyonlinelibrary.com]

efficacy immediately (first FP) decreased with cathodal DCS (−33.5 ± 21%, *n* = 9, *P* < 0.05) and increased with anodal DCS (28.8 ± 26.8%, *n* = 11, *P* < 0.05). The effect of DCS was sustained for the duration of the EF but there is an adaptation to DCS during anodal stimulation (Fig. 5*B*).

DCS promotes synaptic cooperativity through recruitment of afferent axons

The negative correlation between the transient change in FP amplitude and the change in FP amplitude during DCS suggests there is an adaptation to the effect of DCS (Fig. 5*C*). We hypothesized the adaptation to DCS may be attributed to recruitment of presynaptic axons during DCS. EFs along the ascending afferent axons may be polarizing presynaptic compartments leading to recruitment of additional afferents (N_f in eqn (1)) during orthodromic stimulation. We tested this hypothesis by changing the orthodromic stimulation intensity by a half (½×) or by doubling it (2×), thus decreasing or increasing, respectively, the number of afferent fibres generating the field potential. The protocol is similar to the post-adaptation DCS experiment but here the EF is replaced with a change in stimulus intensity.

Both DCS and changes in orthodromic stimulus intensity result in similar dynamics of the FP (Fig. 5*D*). During cathodal DCS and the analogous ½× stimulus intensity experiments, FP amplitudes were transiently depressed and recovered from depression. During anodal DCS and the analogous 2× orthodromic stimulus intensity experiments, FP amplitudes were transiently facilitated and gradually recovered from facilitation towards baseline. In both cathodal DCS and ½× stimulus intensity experiments we observe a prominent rebound in FP amplitude after DCS was turned off and after stimulus intensity was returned to the probing intensity. These results suggest DCS changes the presynaptic axon membrane potential and modulates the sensitivity to firing action potentials. A model incorporating synaptic depression and recruitment is able to capture the salient features of the experimental data (Fig. 5*E*). A single postsynaptic neuron with integrate-and-fire dynamics receives synaptic current from a fixed number of pre-synaptic inputs. The dynamics of the synaptic inputs are modelled using the facilitation–depression model described in the methods (Fig. 1). Recruitment is modelled as an instantaneous increase in the number of active pre-synaptic inputs for the duration of the EF. A DCS-induced postsynaptic depolarization alone fails to capture the non-linear effects of DCS on FP amplitude.

DCS can change synaptic efficacy even without recruitment of afferent fibres during orthodromic stimulation. Axons within L2/3 (L2/3 → 2/3) were orthodromically stimulated while only polarizing the postsynaptic cells. There is a significant immediate change

in FP amplitude (the first FP during the train) during DCS (-20 V m^{-1}: $3.15 \pm 1.18\%$, $n = 5$; $+20$ V m^{-1}: $6.44 \pm 4.78\%$, $n = 5$). The dynamics of recruitment that would have resulted in an offset of the FP amplitude and a recovery from facilitation or depression towards baseline were not observed. This result, along with previously published work, shows postsynaptic polarization alone can modulate synaptic efficacy. However, the immediate change in synaptic efficacy is less than when activating the vertical L5 $\rightarrow$ 2/3 pathway (6.44% *vs.* 28.8% for 20 V m^{-1}), suggesting some of the change in synaptic efficacy we observe during DCS of the L5 $\rightarrow$ 2/3 pathway may result from recruitment of afferent axons.

A change in the fibre volley (FV) amplitude, which is a compound action potential that reflects the number of activated axons, provides direct evidence for recruitment with DCS. EFs along the ascending fibres in motor cortex (L5 $\rightarrow$ 2/3) decreased FV amplitude by $-15.5 \pm 10\%$ with -20 V m^{-1} ($n = 30$) and increased FV amplitude by $13.9 \pm 7.1\%$ with $+20$ V m^{-1} ($n = 30$) (Fig. 7*A*). Similarly, in hippocampal CA1 area, EFs along Schaffer collaterals increased FV amplitude by $10.6 \pm 10.4\%$ ($P < 0.05$) with -20 V m^{-1} ($n = 20$) and decreased FV amplitude by $-5.5 \pm 8\%$ ($P < 0.05$) with $+20$ V m^{-1} ($n = 20$) (Fig. 7*B*). The polarity of modulation during DCS reflects axonal polarization such that depolarized regions of the axon (distal to the positive electrode) correspond to an increase in FV amplitude. In motor cortex, there is a direct positive correlation (r: 0.92, CI: [0.88, 0.95]) between change in FP amplitude and change in FV amplitude. Recruitment of
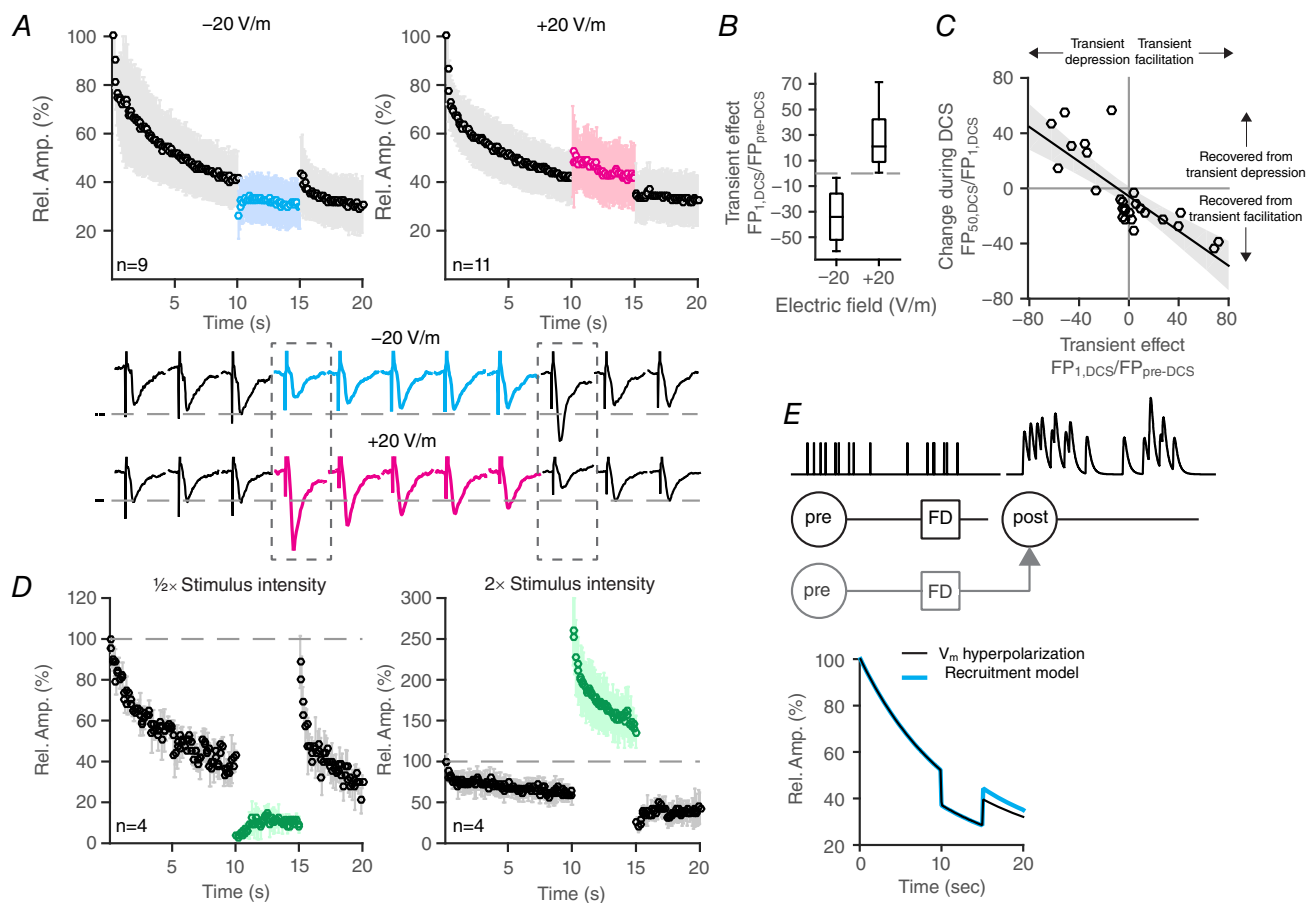
Figure 5. DCS post adaptation modulates synaptic efficacy and is driven by recruitment of afferent axons

A, cathodal (blue) and anodal DCS (magenta) during a train of synaptic inputs at 10 Hz modulates synaptic efficacy for the duration of the electric field (EF) despite adaptation. *B*, DCS polarity specifically modulates the first field potential (FP) amplitude relative to pre-DCS. *C*, there is a correlation between the change in the first FP amplitude and the amount of recovery from facilitation or depression during DCS. *D*, changing the stimulus intensity, instead of applying DCS, results in similar dynamics on FP amplitude. Decreasing stimulus intensity by a half (left) decreases FP amplitudes. There is a pronounced rebound in FP amplitude when the stimulus intensity is returned to the probe intensity. *E*, a simple dynamic synapse model incorporating recruitment of presynaptic inputs is able to reproduce the effects of DCS on synaptic efficacy and the post-DCS rebound effect. [Colour figure can be viewed at wileyonlinelibrary.com]

afferent axons during DCS in brain slices may contribute to the modulation of synaptic activity (Fig. 7*C*).

Discussion

Especially in contrast to techniques such as transcranial magnetic stimulation (TMS) or deep brain stimulation (DBS), the most conspicuous features of tDCS are diffuse, low-intensity, and sustained current flow (Peterchev *et al.* 2011) – and so accounting for these features seems essential to a specific explanation of tDCS mechanisms. Our key results show that DCS produces a sustained modulation of synaptic efficacy that is cumulative over the duration of the EF when applied during ongoing synaptic activity. Ongoing synaptic activity produces well-established changes in synaptic dynamics (Abbott *et al.* 1997; Varela *et al.* 1997; Zucker & Regehr, 2002; Abbott & Regehr, 2004; Richardson *et al.* 2005), with depression dominating in motor cortex. We addressed the question of if/how synaptic dynamics would affect modulation by DCS (Fig. 1). We show synaptic depression contributes to moderate loss in acute sensitivity to DCS (from 1.1% per V m^{-1} to 0.55% per V m^{-1}; Fig. 2*E*). However, there is a significant modulation that is robust across orthodromic stimulation frequency (Fig. 3) and extends to naturalistic input (Fig. 4) and post-adaptation states (Fig. 5). tDCS in humans has been shown to reduce motion after-effects, which are a result of adaptation, potentially arising from synaptic depression or spike rate adaptation (Antal *et al.* 2004; Kar & Krekelberg, 2012). Our results highlight the potential for a lingering effect of DCS that manifests itself in changes to synaptic dynamics.

Importantly, a cumulative gain in synaptic potentials amplifies the DCS effect because the modulation of synaptic efficacy by DCS is sustained (Fig. 2*F*) – ongoing synaptic activity combined with sustained DCS is an important feature of tDCS. In fact, Shu *et al.* (2006) demonstrated that interactions between the presynaptic and postsynaptic action potentials may not be required for strengthening synaptic transmission under conditions when the duration of the presynaptic action potentials is increased through somatic polarization.

We also demonstrate that afferent axon polarization can drive the changes in synaptic activity during DCS (Fig. 7), adjunct to traditional somatic polarization (Fig. 6) and axon terminal mediated mechanisms (Hause, 1975; Rahman *et al.* 2013; Bolzoni *et al.* 2013*b*; Bolzoni & Jankowska, 2015). Thus, a targeted brain region may be influenced by both direct modulation of local neuronal processes and by polarizing afferent brain regions (Bolzoni & Jankowska, 2015; Jankowska *et al.* 2016). The diversity of experimental findings is well quantified by a model of synaptic dynamics (Figs 4 and 5*E*) – though we cannot exclude contributions from additional factors such as changes in polarization sensitivity by active neurons (Antal *et al.* 2004; Reato *et al.* 2010). Although our analysis is for a reduced system, these results have important consequences for how the outcomes of diffuse and weak transcranial electrical stimulation are interpreted, and suggest these features can be advantageous.

tDCS using conventional montages with two large pad electrodes produces diffuse current flow through the cortex and subcortical brain regions (Datta *et al.* 2009; Bikson *et al.* 2010). For example, the common M1–SO tDCS montage (Datta *et al.* 2009) produces diffuse current flow not only on the nominal brain target, but also in premotor and supplementary motor cortex (Fig. 8*A*), in addition to other cortical and subcortical brain regions (Bolzoni *et al.* 2013*a*,*b*; Baczyk & Jankowska, 2014). Consequently, the cellular effects of tDCS are not localized to just the targeted brain region but can extend to upstream brain regions. In this way diffuse tDCS may recruit a distributed brain network, for instance the
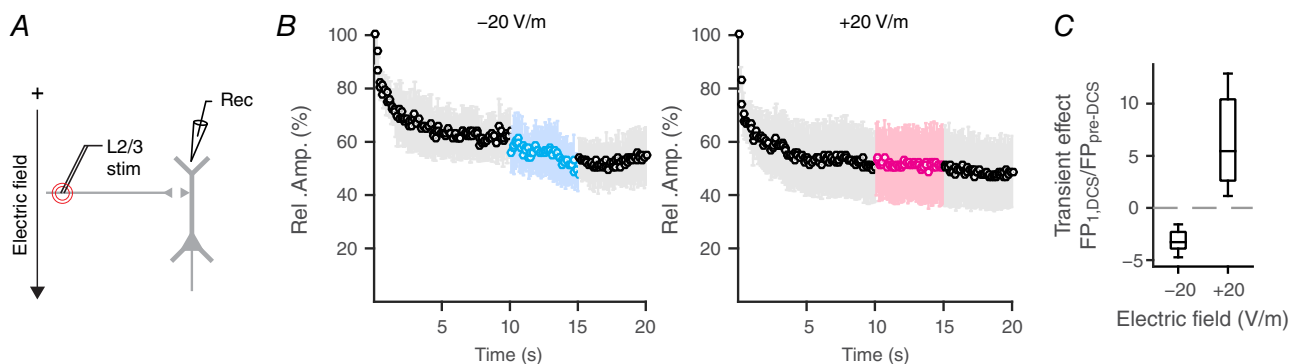
Figure 6. DCS modulates synaptic efficacy post adaptation through somatic polarization alone
*A*, schematic diagram of orthodromic stimulation of L2/3 during DCS. Current flow along the somato-dendritic axis and perpendicular to the horizontally oriented axons selectively polarizes the postsynaptic cells and not the axons. *B*, current flow along the somato-dendritic axis during orthodromic stimulation of the horizontal L2/3 pathway modulates synaptic efficacy independently of axonal recruitment. *C*, anodal DCS facilitates synaptic efficacy and cathodal DCS depresses efficacy. [Colour figure can be viewed at wileyonlinelibrary.com]

network of brain regions involved in motor planning or execution. However, diffusivity in itself is not a substrate for producing specific behavioural or clinical changes, and needs to be considered in the context of endogenous activity between connected brain regions. Modulation of upstream brain regions can influence the cooperative action of neurons and thus directly affect downstream processes.

The notion of diffuse and sustained current flow being advantageous features of tDCS further extends to how the effects of weak electric fields produced by tDCS are amplified by brain activity. The difference between resting membrane potential and spike threshold for a typical cortical pyramidal cell can be 15–20 mV. DCS, however, results in a small change in membrane potential (~ 0.2 mV per V m^{-1}) at the soma. Amplifying synaptic activity through cooperative inputs during DCS provides a mechanism by which weak EFs can significantly modulate the postsynaptic response (eqn (1)). An increase in presynaptic firing rate or the synchronous activation of presynaptic cells during diffuse current flow can directly increase postsynaptic depolarization and firing probability (Fig. 8*A* and *B*). Future *in vitro* experiments to directly test this hypothesis can selectively apply DCS and orthodromic stimulation of afferents in separate brain regions. For instance, one could orthodromically stimulate and polarize with DCS an afferent (upstream) brain region (i.e. premotor) and record the synaptic response in a target brain area (i.e. motor cortex), which was not polarized by DCS. Our hypothesis suggests synaptic responses in the motor cortex will be modulated by changes in the activity of afferent brain regions.

To formalize our hypothesis that diffuse current flow may be advantageous for neuronal information processing, we present a statistical theory (eqn (5)) for increasing synaptic strength through coincident pre- and postsynaptic spikes. We consider the number of presynaptic spikes (N_{pre}) and the number of
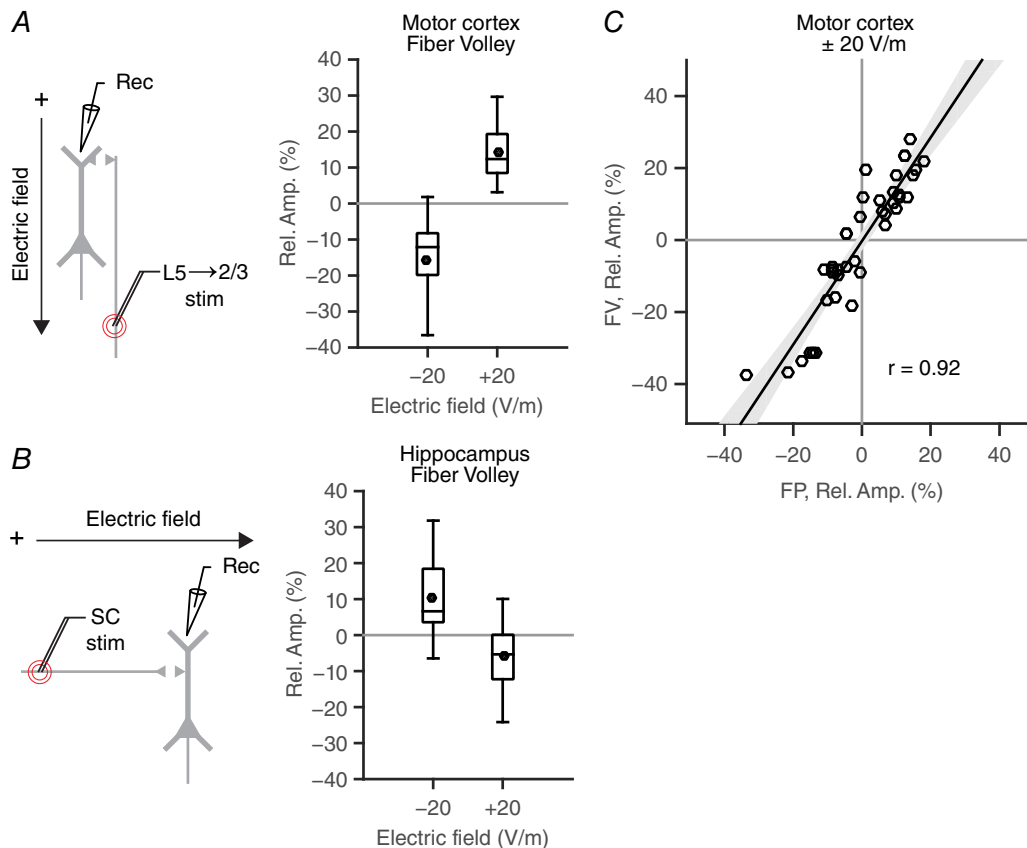
**Figure 7. Current flow along axons during DCS modulates fibre volley in rat primary motor cortex and hippocampus**
A, current flow along the somato-dendritic axis during orthodromic stimulation of the ascending L5 → 2/3 pathway polarizes afferent axons and modulates axonal recruitment during DCS. The amplitude of the fibre volley (FV) reflects the number of axons firing action potentials during orthodromic stimulation. *B*, similarly, current flow along the afferent axons of the Schaffer collateral pathway modulates the fibre volley amplitude. *C*, the change in fibre volley amplitudes is directly correlated with the change in postsynaptic field potential (FP) amplitude in the rat primary motor cortex. These results show polarizing afferent axons changes the number of active presynaptic inputs and directly modulates synaptic current. [Colour figure can be viewed at wileyonlinelibrary.com]

postsynaptic spikes (N_{post}) in discrete time bins (N_{bins}). The hypergeometric distribution estimates the coincidence count probability $P(k|N_{pre}, N_{post}, N_{bins})$ of observing k coincident pre- and postsynaptic spikes from a given number of bins and having observed N_{post} postsynaptic spikes and N_{pre} presynaptic spikes. By varying the number of presynaptic spikes or postsynaptic spikes we have an estimate of the number of coincidences. The probability distribution of coincidences closely matches the true number of coincidences in simulations of neuronal activity (Fig. 8C, dashed vertical line is estimated number of coincidences from simulations of neuronal activity). During tDCS a change in presynaptic firing rate (as a result of diffuse current flow), or postsynaptic firing rate, or both, can increase the coincidence probability and thus promote synaptic strengthening between connected and active brain regions. While weak electric fields cannot induce firing on their own they exert a modulatory effect on active networks and increase the probability of synaptic strengthening. This novel theory is supplementary to well-established direct changes in synaptic efficacy and connectivity (Buch *et al.* 2011; Kabakov *et al.* 2012; Bikson *et al.* 2012*b*).

Ongoing studies in both humans and animals can test the role of neuromodulation of brain regions upstream to the nominal target, according to our quantitative hypothesis. However, it is already established that tDCS produces peak brain current densities are often in between, rather than under the electrodes (Miranda *et al.* 2006; Datta *et al.* 2009; Dasilva *et al.* 2012), meaning diffuse neuromodulation is expected across inter-connected brain regions. Our experimentally constrained statistical theory predicts that tDCS increases presynaptic firing rate (Fig. 5) in a sustained manner (Figs 3 and 4), increasing synaptic integration (Fig. 2F) and the coincidence of pre- and postsynaptic action potentials, which both increase the likelihood of synaptic plasticity (Fig. 8). In this way, combining tDCS with training can enhance

Figure 8. tDCS produces diffuse current flow in the brain which increases the probability of coincident pre- and postsynaptic inputs
A, the electric field magnitude is plotted in a finite element model of tDCS with anode over the primary motor cortex (M1) and cathode over supraorbital region (SO). The electric field magnitude distribution in brain regions adjacent and upstream to M1 is comparable to or higher than in M1. *B*, the primary motor cortex is synaptically connected to the supplementary motor area (SMA) and premotor cortex (PMC), which drives motor activity. The thickness of the arrows indicates the relative connection strength from fMRI studies of this functional network. Modulating presynaptic activity in these upstream brain regions during tDCS may drive postsynaptic activity in M1. *C*, DCS-induced membrane polarization changes the likelihood of firing. An increase in the presynaptic activity (or postsynaptic activity) increases the probability of coincident pre- and postsynaptic action potentials. The vertical grey dashed lines in the graph indicate the simulated number of coincidences in a model Integrate & Fire (I&F) neuron receiving Poisson distributed synaptic inputs. The hypergeometric probability distribution can be used to approximate the estimated number of coincidences. Combined, these results suggest the probability of coincident inputs can be directly modulated when presynaptic or postsynaptic activity is modulated by diffuse current flow. [Colour figure can be viewed at wileyonlinelibrary.com]
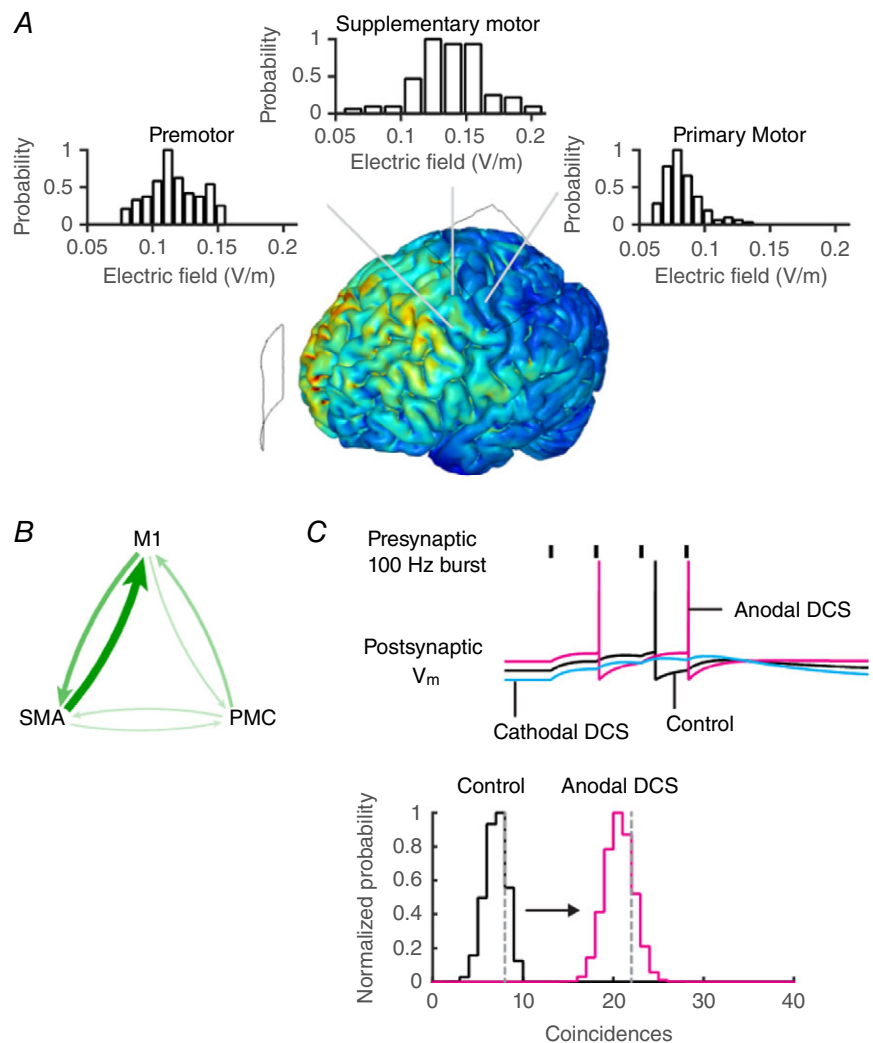
connectivity between those regions activated by training, and potentially enhance the outcomes of training. This theory captures key features of a typical tDCS protocol: tDCS produces diffuse current flow in the brain, needs to be applied for an extended period of time to integrate synaptic activity, and matched to a sustained task (Bikson & Rahman, 2013). The notable prediction of our model is that the diffusivity of tDCS is, in fact, advantageous since polarization of the target (N_{post}), or afferent region (N_{pre}), or optimally both will enhance connectivity.

References

Abbott LF & Regehr WG (2004). Synaptic computation. *Nature* **431**, 796–803.

Abbott LF, Varela JA, Sen K & Nelson SB (1997). Synaptic depression and cortical gain control. *Science* **275**, 220–224.

Antal A, Bikson M, Datta A, Lafon B, Dechent P, Parra LC & Paulus W (2012). Imaging artifacts induced by electrical stimulation during conventional fMRI of the brain. *Neuroimage* **85**, 1040–1047.

Antal A, Varga ET, Kincses TZ, Nitsche MA & Paulus W (2004). Oscillatory brain activity and transcranial direct current stimulation in humans. *Neuroreport* **15**, 1307–1310.

Baczyk M & Jankowska E (2014). Presynaptic actions of transcranial and local direct current stimulation in the red nucleus. *J Physiol* **592**, 4313–4328.

Bikson M, Datta A, Rahman A & Scaturro J (2010). Electrode montages for tDCS and weak transcranial electrical stimulation: role of "return" electrode's position and size. *Clin Neurophysiol* **121**, 1976–1978.

Bikson M, Dmochowski J & Rahman A (2012*a*). The "quasi-uniform" assumption in animal and computational models of non-invasive electrical stimulation. *Brain Stimul* **6**, 704–705.

Bikson M, Inoue M, Akiyama H, Deans JK, Fox JE, Miyakawa H & Jefferys JG (2004). Effects of uniform extracellular DC electric fields on excitability in rat hippocampal slices *in vitro*. *J Physiol* **557**, 175–190.

Bikson M & Rahman A (2013). Origins of specificity during tDCS: anatomical, activity-selective, and input-bias mechanisms. *Front Hum Neurosci* **7**, 688.

Bikson M, Reato D & Rahman A (2012*b*). Cellular and network effects of transcranial direct current stimulation: insights from animal models and brain slice. In *Transcranial Brain Stimulation*, 1st edn, eds Miniussi C, Paulus W & Rossini PM, pp. 55–91. CRC Press, New York

Bolzoni F, Baczyk M & Jankowska E (2013*a*). Subcortical effects of transcranial direct current stimulation in the rat. *J Physiol* **591**, 4027–4042.

Bolzoni F & Jankowska E (2015). Presynaptic and postsynaptic effects of local cathodal DC polarization within the spinal cord in anaesthetized animal preparations. *J Physiol* **593**, 947–966.

Bolzoni F, Pettersson LG & Jankowska E (2013*b*). Evidence for long-lasting subcortical facilitation by transcranial direct current stimulation in the cat. *J Physiol* **591**, 3381–3399.

Buch ER, Johnen VM, Nelissen N, O'Shea J & Rushworth MF (2011). Noninvasive associative plasticity induction in a corticocortical pathway of the human brain. *J Neurosci* **31**, 17669–17679.

Dasilva AF, Mendonca ME, Zaghi S, Lopes M, Dossantos MF, Spierings EL, Bajwa Z, Datta A, Bikson M & Fregni F (2012). tDCS-induced analgesia and electrical fields in pain-related neural networks in chronic migraine. *Headache* **52**, 1283–1295.

Datta A, Bansal V, Diaz J, Patel J, Reato D & Bikson M (2009). Gyri-precise head model of transcranial direct current stimulation: Improved spatial focality using a ring electrode versus conventional rectangular pad. *Brain Stimulation* **2**, 201–207.

Hause L (1975). A mathematical model for transmembrane potentials secondary to extracellular fields. In *Electroanaesthesia: Biomedical and Biophysical Studies*, eds Sances J & Larson S, pp. 176–200. Academic Press, New York.

Hultborn H, Illert M, Nielsen J, Paul A, Ballegaard M & Wiese H (1996). On the mechanism of the post-activation depression of the H-reflex in human subjects. *Exp Brain Res* **108**, 450–462.

Jackson MP, Rahman A, Lafon B, Kronberg G, Ling D, Parra LC & Bikson M (2016). Animal models of transcranial direct current stimulation: Methods and mechanisms. *Clin Neurophysiol* **127**, 3425–3454.

Jankowska E, Kaczmarek D, Bolzoni F & Hammar I (2016). Evidence that some long-lasting effects of direct current in the rat spinal cord are activity-independent. *Eur J Neurosci* **43**, 1400–1411.

Jefferys JGR (1981). Influence of electric fields on the excitability of granule cells in guinea-pig hippocampal slices. *J Physiol* **319**, 143–152.

Kabakov AY, Muller PA, Pascual-Leone A, Jensen FE & Rotenberg A (2012). Contribution of axonal orientation to pathway-dependent modulation of excitatory transmission by direct current stimulation in isolated rat hippocampus. *J Neurophysiol* **107**, 1881–1889.

Kar K & Krekelberg B (2012). Transcranial electrical stimulation over visual cortex evokes phosphenes with a retinal origin. *J Neurophysiol* **108**, 2173–2178.

Krishnamurthy V, Gopinath K, Brown GS & Hampstead BM (2015). Resting-state fMRI reveals enhanced functional connectivity in spatial navigation networks after transcranial direct current stimulation. *Neurosci Lett* **604**, 80–85.

Marquez-Ruiz J, Leal-Campanario R, Sanchez-Campusano R, Molaee-Ardekani B, Wendling F, Miranda PC, Ruffini G, Gruart A & Delgado-Garcia JM (2012). Transcranial direct-current stimulation modulates synaptic mechanisms involved in associative learning in behaving rabbits. *Proc Natl Acad Sci USA* **109**, 6710–6715.

Miranda PC, Lomarev M & Hallett M (2006). Modeling the current distribution during transcranial direct current stimulation. *Clin Neurophysiol* **117**, 1623–1629.

Mongillo G, Barak O & Tsodyks M (2008). Synaptic theory of working memory. *Science* **319**, 1543–1546.

Nitsche MA & Paulus W (2000). Excitability changes induced in the human motor cortex by weak transcranial direct current stimulation. *J Physiol* **527**, 633–639.

Peterchev AV, Wagner TA, Miranda PC, Nitsche MA, Paulus W, Lisanby SH, Pascual-Leone A & Bikson M (2011). Fundamentals of transcranial electric and magnetic stimulation dose: definition, selection, and reporting practices. *Brain Stimul* **5**, 435–453.

Polania R, Nitsche MA & Paulus W (2011). Modulating functional connectivity patterns and topological functional organization of the human brain with transcranial direct current stimulation. *Hum Brain Mapp* **32**, 1236–1249.

Polania R, Paulus W & Nitsche MA (2012). Modulating cortico-striatal and thalamo-cortical functional connectivity with transcranial direct current stimulation. *Hum Brain Mapp* **33**, 2499–2508.

Priori A (2003). Brain polarization in humans: a reappraisal of an old tool for prolonged non-invasive modulation of brain excitability. *Clin Neurophysiol* **114**, 589–595.

Radman T, Ramos RL, Brumberg JC & Bikson M (2009). Role of cortical cell type and morphology in subthreshold and suprathreshold uniform electric field stimulation *in vitro*. *Brain Stimul* **2**, 215–228.

Rahman A, Lafon B & Bikson M (2015). Multilevel computational models for predicting the cellular effects of noninvasive brain stimulation. *Prog Brain Res* **222**, 25–40.

Rahman A, Reato D, Arlotti M, Gasca F, Datta A, Parra LC & Bikson M (2013). Cellular effects of acute direct current stimulation: somatic and synaptic terminal effects. *J Physiol* **591**, 2563–2578.

Reato D, Rahman A, Bikson M & Parra LC (2010). Low-intensity electrical stimulation affects network dynamics by modulating population rate and spike timing. *J Neurosci* **30**, 15067–15079.

Richardson MJ, Melamed O, Silberberg G, Gerstner W & Markram H (2005). Short-term synaptic plasticity orchestrates the response of pyramidal cells and interneurons to population bursts. *J Comput Neurosci* **18**, 323–331.

Shu Y, Hasenstaub A, Duque A, Yu Y & McCormick DA (2006). Modulation of intracortical synaptic potentials by presynaptic somatic membrane potential. *Nature* **441**, 761–765.

Stagg CJ, Lin RL, Mezue M, Segerdahl A, Kong Y, Xie J & Tracey I (2013). Widespread modulation of cerebral perfusion induced during and after transcranial direct current stimulation applied to the left dorsolateral prefrontal cortex. *J Neurosci* **33**, 11425–11431.

Tsodyks MV & Markram H (1997). The neural code between neocortical pyramidal neurons depends on neurotransmitter release probability. *Proc Natl Acad Sci USA* **94**, 719–723.

Varela JA, Sen K, Gibson J, Fost J, Abbott LF & Nelson SB (1997). A quantitative description of short-term plasticity at excitatory synapses in layer 2/3 of rat primary visual cortex. *J Neurosci* **17**, 7926–7940.

Zucker RS & Regehr WG (2002). Short-term synaptic plasticity. *Annu Rev Physiol* **64**, 355–405.

Additional information

Competing interests

M.B. and L.P. have equity in Soterix Medical Inc. The City University of New York has patents on brain stimulation with M.B. and L.P. as inventors.

Author contributions

A.R. and M.B. contributed to the conception and design of the work, acquisition, analysis, and interpretation of data for the work and drafting the work. B.L. and L.P. contributed to revising it critically for important intellectual content and interpretation of data for the work. All authors approved the final version of the manuscript and agree to be accountable for all aspects of the work in ensuring that questions related to the accuracy or integrity of any part of the work are appropriately investigated and resolved. All persons designated as authors qualify for authorship, and all those who qualify for authorship are listed.

Funding